Polarimetry: From the Sun to Stars and Stellar Environments
Proceedings IAU Symposium No. 305, 2014
K. N. Nagendra, S. Bagnulo, R. Centeno &
M. J. Martínez González, eds.

doi:10.1017/S1743921315004871

Circumstellar Polarimetry

A. M. Magalhães, A. C. Carciofi and D. B. Seriacopi

Departamento de Astronomia, IAG, Universidade de São Paulo, Rua do Matão 1226, São Paulo, SP 05508-090, Brazil
email: antonio.mario@iag.usp.br

Abstract. Starlight polarization provides insight into the physical mechanisms in and around the source as well as its geometry, whether or not the source is resolved. In this talk we will review mechanisms that polarize light in stellar envelopes. The observations and modeling can be used to probe the physics of the circumstellar environment as well as its relation to the ambient interstellar environment.

Keywords. Polarization, radiative transfer, scattering, stars: atmospheres, stars: circumstellar matter, techniques: polarimetric

1. Introduction

Observations of stellar polarimetry provide important information about the physical mechanisms operating in and around the source as well as the source's asymmetry. A powerful feature of the technique is that the source does not have to be angularly resolved, which is often the case for stellar envelopes, especially outside the Milky Way.

In the context of circumstellar envelopes, mechanisms that polarize light include Rayleigh scattering from atoms and molecules, Mie (i.e., dust) scattering and Thompson scattering by free electrons. A spherical envelope of any such scatterers produces no net polarization; an observed non-zero polarization (after a possible interstellar polarization subtraction) signals the presence of a non-spherical envelope.

One such example is that of a hot star surrounded by an unresolved, ionized, non-spherical envelope, such as those around Be and B[e] stars. The observer receives direct (i.e., mostly unpolarized) stellar flux as well as flux which has been scattered (hence polarized to some extent) within the envelope. The observed degree of polarization is essentially the ratio between the scattered and total flux. Most importantly, the polarized flux conveys information about the emission and absorption processes that occur in the envelope. Be stars (Bjorkman 2006) are one such example, where line absorption, barely noticeable in total flux, may be quite evident in the polarization spectrum (sec. 3.1.1).

As stellar sub-milimeter astronomy becomes more and more mainstream, a technique that may become more popular is the study of thermal emission by circumstellar dust grains. Such emission from, say, a non-spherical envelope of aligned grains will be polarized. Sub-mm polarimetry is already important in the context of star formation and the magnetic field structure in the parent dust cloud (e.g., Stephens *et al.* 2013; Hull, this volume). This will not be discussed here but, as the technology evolves, emission polarization from circumstellar envelopes (e.g., with ALMA) will likely see more widespread use.

In this article, we aim mostly at exemplifying the kinds of physical information that one can gather from circumstellar polarimetry observations and basic principles. No attempt is made to make a full review of the rather extensive literature on the topic.

2. Polarizing Mechanisms

2.1. *Electron scattering*

In scattering by free electrons (e.g., Rybicki & Lightman 1985), or Thompson scattering, the scattered intensity per electron per unit incident flux into a unit solid angle is

$$d\sigma/d\Omega = \frac{1}{2} r_0^2 (1 + \cos^2\theta) = \frac{3}{16\pi} \sigma_T (1 + \cos^2\theta) \tag{2.1}$$

where σ_T is the Thompson cross section and θ is the scattering angle from the initial direction. The linear polarization from such scattering is

$$p(\theta) = \frac{(1 - \cos^2\theta)}{(1 + \cos^2\theta)} \tag{2.2}$$

.

The Thompson cross section, $\sigma_T = \frac{8\pi}{3} r_0^2 = 6.65 \times 10^{-25} cm^2$, where $r_0 = \frac{e^2}{mc^2} =$ *classical electron radius*, is wavelength independent. It is instructive however to consider the broader case of electron scattering.

Take a two-level atom with a bound electron. For photon frequencies much lower than the frequency of the transition, ω_0, the electron cross section will be $\sigma(\omega) \approx \sigma_T \left(\frac{\omega}{\omega_0}\right)^4$. This is Rayleigh scattering, responsible for the blue of the sky. This is also a source of scattering opacity (e.g., from H and He atoms) in cool star atmospheres.

At frequencies near the resonance, or $\omega \approx \omega_0$, the cross section has the familiar Lorenzian shape, $\sigma(\omega) = \sigma_T \frac{\omega^4}{(\omega^2 - \omega_0^2)^2 + (\omega_0^3 \tau)^2}$, where $\Gamma = \omega_0^2 \tau$ is the natural resonance width. Classically, the Lorenzian absorption shape comes from the Fourier transform of the damped, radiating oscillator. One familiar example are lines from atmospheric O_2 and N_2 molecules in the near UV, where $\omega_0 \approx 6 \times 10^{15} Hz$.

Finally, at frequencies well above ω_0, $\sigma(\omega) = \sigma_T$, the free electron value, up to frequencies $\approx c/r_0 \approx 10^{23} Hz$. In the X-ray regime classical theory ceases to be valid. In this frequency range the Klein-Nishina total and differential cross sections apply; $\sigma(\omega)$ then ranges from $\sim \sigma_T$ to $\sim 1/10\ \sigma_T$ for photon energies of about 1/100 to 10 $m_e c^2$, respectively.

It is remarkable that Thompson scattering, with such a relatively small cross section, plays a crucial role in polarization phenomena ranging from hot star disks, AGN, galaxy clusters and the Cosmic Microwave Background!

2.2. *Dust*

Dust is also ubiquitous in the Universe, being a tracer of star formation from within our Galaxy and the Local Group out to the first galaxies at high redshift. While cross sections can be now calculated for almost any particle size and shape (Draine 2011), a lot can still be understood by considering spherical particles. This particular problem has been solved by Mie (1908).

In this case (van de Hulst 1981), the cross sections will depend on $x = 2\pi a/\lambda$, the particle size, a, measured in terms of the wavelength, λ, of the incoming radiation, as well as the particle material, expressed through its complex index of refraction, $m(\lambda)$. A non-zero imaginary part of $m(\lambda)$ indicates that the particle will absorb a fraction of the incoming radiation; this means that there will now be both scattering and absorption cross sections. The extinction cross section is the sum of these two. Also, the real part of $m(\lambda)$ will change the phase of the incoming wave; this means that incident linearly polarized radiation may become circularly polarized after scattering, something which cannot happen with electron scattering.

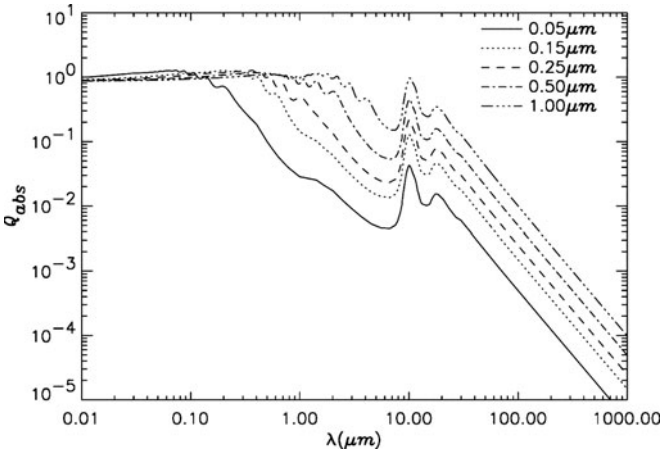

Figure 1. Absorption coefficients for silicate dust particles of various sizes. From Carciofi, Bjorkman & Magalhães (2004).

One can think of the incoming radiation as exciting the various multipoles inside the dust particle (van de Hulst 1981). When $x \ll 1$, i.e., small particles compared to the wavelength (the Rayleigh domain), the electric dipole term dominates and the cross sections are

$$\sigma_{sca,Ray} = \frac{2}{3}\pi^5 \frac{(2a)^6}{\lambda^4}\left|\frac{m^2-1}{m^2+2}\right|^2, \qquad \sigma_{abs,Ray} = \pi\left(\frac{(2a)^3}{\lambda}\right) Im\left(\frac{m^2-1}{m^2+2}\right) \tag{2.3}$$

.

One can note that the wavelength behavior of $\sigma_{sca,Ray}$ is identical to that of atomic/molecular Rayleigh scattering (sec. 2.1). In general however, for an arbitrary grain size many multipoles contribute to the scattering and extinction cross sections and the expressions become, respectively,

$$\sigma_{sca} = \frac{2\pi}{k^2}\sum_{n=1}^{\infty}(2n+1)\left(|a_n|^2+|b_n|^2\right), \qquad \sigma_{ext} = \frac{2\pi}{k^2}\sum_{n=1}^{\infty}(2n+1)Re(a_n+b_n), \tag{2.4}$$

where k is the wavenumber. The Mie expansion coefficients a_n and b_n can be calculated in terms of the Ricatti-Bessel functions, which are essentially spherical Bessel functions, with arguments x and mx. Figure 1 (Carciofi, Bjorkman & Magalhães 2004) shows absorption factors, defined as $Q_{abs} = \sigma_{abs}/\pi a^2$, for silicate particles of various sizes. Q_{ext} and Q_{sca} are similarly defined, where $Q_{ext} = Q_{abs} + Q_{sca}$.

Bruce Draine's page (http://www.astro.princeton.edu/∼draine/scattering.html) includes several useful codes, including Bohren & Huffman's code (Bohren & Huffman 1998) for calculating the Mie's absorption and extinction factors. Extinction being higher in the UV/optical/near-infrared (Figure 1), dust around stars absorbs photons at these wavelengths and emits in the mid-IR/far-IR/sub-mm (Figure 2) according to the temperature it attains.

A useful database for optical constants for various materials is one by the U. Jena's Astrophysical Laboratory Group: http://www.astro.uni-jena.de/Laboratory/Database/databases.html.

2.3. *Cyclotron emission*

Cataclysmic variables (CVs) are close binaries consisting of a white dwarf (WD), the primary, and a late-type main-sequence star. The latter fills its Roche lobe and loses

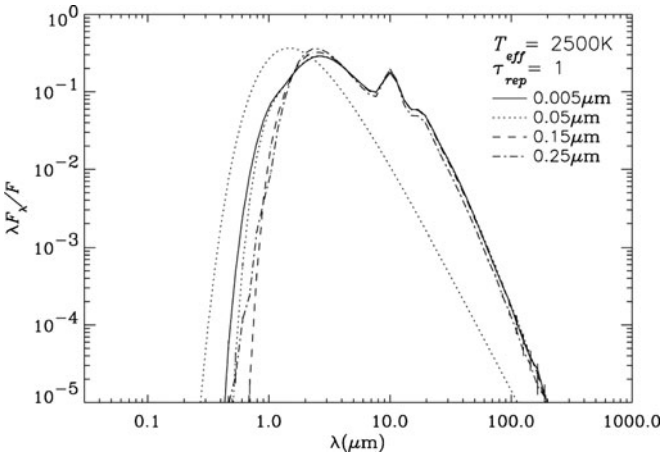

Figure 2. Monte Carlo simulations were used to obtain the spectral energy distribution of four envelope models of the silicate grains in Figure 1, with a = 0.005, 0.05, 0.15, and 0.25 μm surrounding a 2500 K temperature star. For each model, the optical depth was adjusted so that about 63% of the input energy into the dust envelope was absorbed (indicated by $\tau_{rep} = 1$). Also shown is the stellar spectrum (dotted line). From Carciofi, Bjorkman & Magalhães (2004).

material to the WD by the inner Lagrangian point, L1. Due to its angular momentum and viscous processes, this material forms an accretion disk around the WD.

Polars, also called AM Her systems, are CVs without disks. The disks are inhibited by the strong magnetic field of the primary which ranges from 10 to 200 MG at the WD surface. Here, a good fraction of the emission detected in the optical and near-IR is cyclotron radiation, i.e., that of thermal electrons gyrating in a magnetic field. The reader is referred to Silva, Rodrigues, Costa, *et al.* (2013) for further details on these extreme systems, where the accreting region on the WD can be a small fraction of the Earth's radius (!).

2.4. *Modeling*

Solving the radiative transfer of stellar light through the circumstellar envelope is generally performed using the Monte Carlo (MC) method. In this simulation one follows the photon packet's polarization after each scattering by applying a 4x4 Muller matrix to the Stokes vector of the incoming packet (Code & Whitney 1995). The literature in this field is relatively large. Whitney (2011) is a nice introduction to the subject. Her home page, http://gemelli.colorado.edu/∼bwhitney/codes/codes.html, contains code and other useful information.

Carciofi, Bjorkman & Magalhães (2004) discussed the spectral energy distribution of dusty circumstellar envelopes using the MC method. Figure 2 is an example of the resulting spectral energy distribution (SED) from a star surrounded by a dust envelope (in this case, one which reprocesses, or absorbs, 63.2% of the stellar radiation).

An example of a similar MC run where the SED and the spectral polarization are obtained is shown below in sec. 3.3.

2.5. *Measuring the Stokes Parameters*

Circumstellar polarization values of unresolved sources are of the order of a few percent, and often smaller than that. Magalhães *et al.* (1996) and Magalhães (2012) have described an accurate observing technique for the optical/near-infrared which relies on using a rotating waveplate followed by a double-calcite prism ahead of the CCD detector. The

reader is referred to these works for more detail. Section 4 describes a forthcoming survey of the Southern sky which will use the same technique with a robotic telescope.

A separate issue observers have to deal with is correcting their data by the interstellar polarization contribution. This important aspect is discussed virtually by every observational paper mentioned in this article; the reader is referred to them for details (e.g., Wisniewski *et al.* 2010).

The forthcoming ability of ALMA to fully perform polarimetry, mentioned in Section 1, is being nicely complemented in the optical/near-infrared with the start of operation of the imaging and spectro-polarimeter VLT/SPHERE at ESO in 2015. Please check the newsletters and websites of these two observatories for updated information. These will be truly game-changing tools for high resolution studies of stellar atmospheres and their circumstellar environment.

3. Some observational cases

3.1. *Be Stars*

3.1.1. *Disks*

Disks around Be stars are the prototypical scenario among objects with circumstellar material which produce polarization. The early studies of interstellar polarization in the 50's already showed that early-type stars with emission lines often possessed intrinsic polarization.

The cause of the observed linear polarization was correctly attributed to Thompson scattering in a non-spherical envelope. While the electron cross section is wavelength independent, the continuum polarization in Be stars shows wavelength dependence due to absorption and emission processes in the disk (Fig. 3). Polarized scattered light can be attenuated by hydrogen bound-free opacity and/or diluted by hydrogen free-bound emission. In particular, the spectral dependence of the hydrogen bound-free opacity, $\sigma_{bf} \propto \nu^{-3}$ in between ionization edges, produces a rise in polarization from longer wavelengths (where σ_{bf} is highest) to shorter ones (where it is lowest).

Early models (e.g., Capps, Coyne & Dick 1973; McLean 1979; Cassinelli, Nordsieck & Murison 1987) have used single-scattering approximation to model such wavelength dependence, incorporating the above physics. The polarization is essentially the ratio between the scattered, polarized flux and the total flux from the object. The latter includes the attenuated plus scattered stellar flux ($=S_\lambda$) and the emission from the disk ($=D_\lambda$). The polarization can then be written as (Capps, Coyne & Dick 1973)

$$P_\lambda = \frac{f_p f_s S_\lambda}{S_\lambda (e^{-\tau} + f_s) + D_\lambda}, \tag{3.1}$$

where $f_s S_\lambda$ and $f_s f_p S_\lambda$, the scattered and polarized fluxes, respectively, can be expressed using equations 2.1 and 2.2 and the envelope's optical depth, τ, for electron scattering. At temperatures $\approx 10^4$ K, H bound-free emission (which contributes to D_λ) dominates free-free emission in the Balmer continuum (e.g., Draine 2011). At longer wavelengths, such as in the near-infrared, free-free becomes more important.

Fig. 3 shows that the optical/near-UV polarization of ζ Tau (Bjorkman *et al.* 1991) has several of the characteristics of Be polarization expressed by eq. (3.1). The polarization level is typically ≈1%-2%, hinting at the fraction of the stellar light which is scattered by the envelope. The "sawtooth" wavelength dependence of %P described early in this section is also evident in the figure, rising in the optical towards the Balmer discontinuity. The UV WUPPE data in fig. 3 surprisingly showed a lack of rise in %P shortward of the

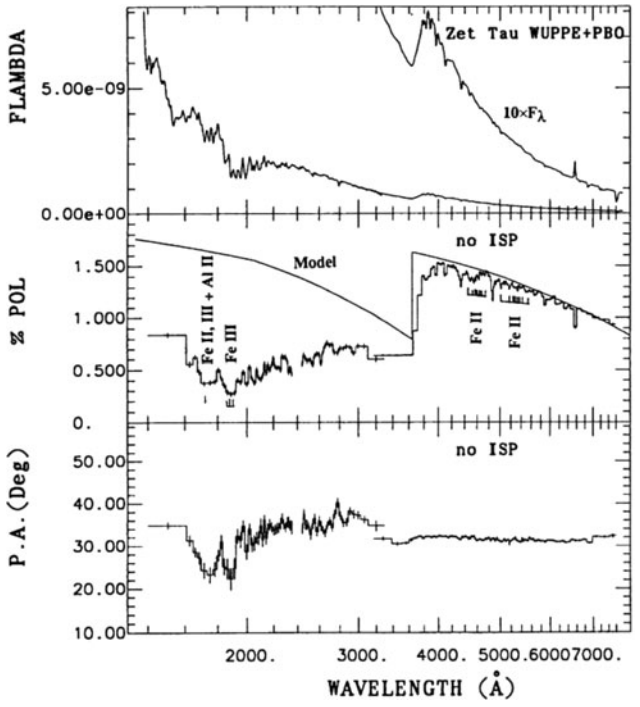

Figure 3. Spectropolarimetry of ζ Tau. The optical data has been taken with HPOL, the U. Wisconsin spectropolarimeter, currently at U. Toledo. The UV data is from the UW's WUPPE experiment on board the Astro-1 observatory. The solid line is a model from Cassinelli, Nordsieck & Murison (1987). From Bjorkman, Nordsieck, Code, *et al.* (1991).

Balmer discontinuity into the UV, attributed to Fe II & Fe III absorption in the envelope. The *optical* spectropolarimetry also showed drops in %P across Fe II lines presumably due to absorption effects, since any dilution in %P by emission is expected to be small.

Wood, Bjorkman & Bjorkman (1997) (WBB) have studied the effects of multiple scattering in the polarization from an axisymmetric electron scattering envelope. They examined how the Be disk opening angle could be constrained. They found that, in addition to raising the overall polarization, multiple scattering plus a wavelength-dependent absorption yielded larger ($\approx$2 $\times$) polarization jumps across the Balmer edge. This resulted in a steeper slope of the polarized continuum compared to single-scattering. This is nicely illustrated by McDavid (2001), who made a detailed comparison between the single and multiple scattering models. Single scattering models provide a good estimate of the spectral polarization up to a value of $\tau \approx 1$ for the radial optical depth τ of the envelope. For comparison, for ζ Tau WBB's best fit gives $\tau = 3$.

Both single scattering (when appropriate) and multiple scattering models show that the Be disks are geometrically thin (i.e., opening angle of a few degrees). The optical polarization in either case is produced within a few (≈ 5) stellar radii from the central star (Carciofi 2012). For comparison, $H\alpha$ emission is produced from ≈ 5 to 20 stellar radii.

3.1.2. *Disk Variability*

Carciofi, Magalhães, Leister, *et al.* (2007) presented the results of a high-accuracy ($\sigma_P \approx 0.005\%$) polarization monitoring of the Be star Achernar (α Eri). They detected variations both in the polarization level and position angle on timescales as short as

1 hr and as long as several weeks. Detailed MC modeling suggested that the short-term variations originated from discrete mass ejection events (i.e., blobs) while long-term variations could be explained by the formation of an inner ring following one or several blob ejection events. Blobs in other hot star winds have also been noted and modeled earlier (Rodrigues & Magalhães 2000).

Be stars are known to occasionally transition from a circumstellar disk ('Be phase') to a state in which evidence for disks disappears ('normal B-star phase'). Wisniewski *et al.* (2010) presented a comprehensive spectropolarimetric monitoring of such a transition for two Be stars, π Aquarii and 60 Cygni. The disk-loss episode of 60 Cyg, for example, was characterized by a generally monotonic decrease in emission strength over a timescale of $\approx$1000 days from the maximum V-band polarization to the minimum $H\alpha$ equivalent width. Interestingly, there existed an observed time lag between the behavior of the polarization and the H emission in both stars, with %P disappearing first. Since we know that %P is produced closer to the star and $H\alpha$ is much more extended (sec. 3.1.1), this lag indicated that the disk clearing proceeded in an 'inside-out' manner.

From the position angles of the intrinsic polarization line in the Q-U plane for each star, Wisniewski *et al.* (2010) have directly determined the orientation of each stellar disk on the sky. Finally, they also observed deviations from the mean intrinsic polarization position angle during polarization outbursts in each star, indicating deviations from axi-symmetry, possibly due to the injection of new blobs into the inner disk, as discussed for Achernar early in this Section.

During each of the five polarimetric outbursts which interrupted these disk-loss events, Draper *et al.* (2011) found that the ratio of the polarization across the Balmer jump versus the V-band polarization traces a distinct loop structure as a function of time. Since the polarization change across the Balmer jump is a tracer of the largest, innermost disk densities whereas the V-band polarization is a tracer of the total scattering mass of the disk, such correlated loop structures in Balmer jump/V-band polarization diagrams (BJV diagrams) provide a unique diagnostic of the radial distribution of mass within Be disks.

3.2. *Wolf-Rayet Stars*

Light scattering by electrons in the winds of a Wolf-Rayet (WR) star is another source of polarized light. A net linear polarization can hence arise if the wind is non-spherically symmetric or the WR star is a member of a binary system, often with an O-type companion. The polarization will typically be time dependent and provide information on the wind structure. Binary WR data can provide additional information, such as physical and geometrical parameters of the system (e.g., St-Louis *et al.* 1993). This is because the WR's companion acts as a source of light which is scattered by the WR wind as a whole. The observed polarization will then vary according to how the WR is viewed as it traces its orbit, producing loops in the Q-U diagram.

Rodrigues & Magalhães (1995) have developed and applied an MC code to model the optical light curve and linear polarization of the WR binary V444 Cyg, an eclipsing WN5+O6 system in a circular orbit. The model fit provides the individual stellar radii, semi-major axis, luminosity ratio, WR wind density and WR mass loss rate.

Some isolated Wolf-Rayet stars present random variability in their optical flux and polarization. Assuming that such variability is caused by blobs in their envelopes, the MC simulations of Rodrigues & Magalhães (2000) showed that the density enhancements must have a large geometric cross section ($\approx$1 stellar radius) and the blobs must be located near the base of the envelope. These sizes are the same inferred from the widths of the sub-peaks in optical emission lines of Wolf-Rayet stars. Other early-type stars

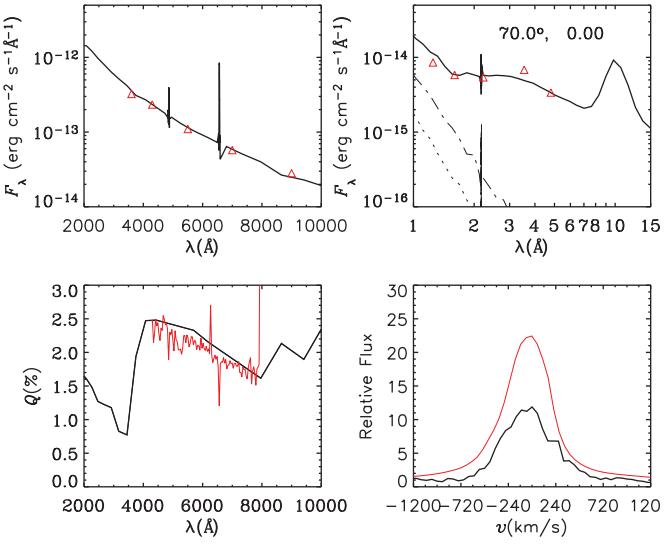

Figure 4. From the upper panels to the lower ones, from left to right: optical flux, IR Flux, optical polarization and Hα profile. The mass loss varies from the pole to the equator, with a disk opening angle (where the mass loss rate is half of that at the equator) of 5°. The gas velocity was taken as purely radial following a latitude-dependent beta-law. The inferred mass loss rates were $3.0 \times 10^{-7} M_{\odot} yr^{-1} sr^{-1}$ and $1.5 \times 10^{-5} M_{\odot} yr^{-1} sr^{-1}$ at the pole and equator, respectively. Polarization is mostly produced by electron scattering in the equatorial disk. From Daiane, Magalhães & Carciofi (2015). See on-line edition of this book for a color version of this figure.

show random polarimetric fluctuations with characteristics similar to those observed in Wolf-Rayet stars, which may also be interpreted in terms of a clumpy wind.

3.3. *B[e] Stars*

Among the classes that populate the hot, luminous part of the H-R diagram, we find the W-R stars, the LBVs and the B[e] stars. While there is evidence to believe that the LBVs are progenitors of the W-R stars (e.g., Maeder & Meynet 2012), the relation of the B[e] stars to these groups and to the evolution of massive stars in general is less clear.

A non-spherical wind model, namely, the two-component model of Zickgraf *et al.* (1985), has become a paradigm for the circumstellar environment of the B[e] supergiants. Further out in their envelopes, at $\approx 10^3$ stellar radii, dust forms close to the equatorial disk and is responsible for near/mid/far IR emission.

The first observations of the optical broadband linear polarization of B[e]SG in the Magellanic Cloud have been reported by Magalhães (1992). The Magellanic character of these rare objects is important due to their known luminosity and confirmed supergiant nature. Magalhães (1992) detected intrinsic polarization in most of them and showed that the data were consistent with the Magellanic B[e]SG having non-spherically symmetric envelopes with a range of intrinsic polarizations. They were also consistent with the spectroscopic data: stars viewed nearly edge-on showed the largest polarizations. Magalhães, Melgarejo, Pereyra, *et al.* (2006) have discussed further diagnostics provided by polarization measurements. Pereyra, Arajo, Magalhães, *et al.* (2009) have used spectropolarimetry across $H\alpha$ (see also Vink, Harries & Drew 2005) to detect the disk of the Galactic B[e] GG Car.

Figure 4 shows observations (triangles & thin red lines) and model results (black lines) for the Magellanic B[e]SG R82 (Daiane, Magalhães & Carciofi 2015). The physical MC model HDUST (Carciofi, Bjorkman & Magalhães 2004; Carciofi & Bjorkman 2006) was used. The model solves for the temperature, ionization structure and population levels of the hydrogen in the disk and incorporates the radiative transfer through the dust envelope further out. Figure 4 exemplifies the near/mid-infrared dust emission (upper right panel) discussed in sec. 2.4 as well as the disk polarization profile (lower left panel) discussed in sec. 3.1.1.

HDUST is further described in Carciofi, Miroshnichenko & Bjorkman (2010), where it was successfully applied to the *Galactic* B[e] star IRAS 00470+6429.

3.4. *Young Stellar Objects*

As mentioned in sec. 2.2 and further exemplified in sec. 3.3, dust is a major constituent of circumstellar matter, especially within star formation regions and in young stars, massive or not, and around evolved objects.

As an example of the science that can be done with polarization by scattering in young objects, we can consider Herbig Ae/Be stars (Rodrigues *et al.* 2009). They present a study of the correlation between the direction of the symmetry axis of the circumstellar material, as evidenced by the intrinsic polarization, around intermediate mass young stellar objects and that of the interstellar magnetic field. They employed CCD polarimetric data on 100 Herbig Ae/Be stars. A large number of them showed intrinsic polarization, indicating non-spherical circumstellar envelopes. The interstellar magnetic field direction was estimated from the polarization of field stars. Rodrigues *et al.* (2009) show that there is an alignment between the position angle of the Herbig Ae/Be star polarization and that of the field stars for the more highly polarized objects. This may be an evidence that the ambient interstellar magnetic field plays a role in shaping the circumstellar material around young stars of intermediate mass and/or in defining their angular momentum axis.

Study of individual objects of this sample can also be revealing. Pereyra, Rodrigues & Magalhães (2012) have studied the PDS 144 N/S binary system, whose optical polarization had been measured by Rodrigues *et al.* (2009). Figure 5 shows the observed optical and NIR polarization vectors on the left, including those of the ambient field. The inset on the right shows the objects as seen using the adaptive optics observations of Perrin *et al.* (2006), with the intrinsic NIR polarization vectors superposed.

Several facts become immediately apparent. First, the intrinsic vectors are aligned with those of the ambient magnetic field. Second, the polarization vector of PDS144 N is perpendicular to the resolved disk structure of the star. These two facts are entirely consistent with the findings of Rodrigues *et al.* (2009). Third, the polarization vectors are remarkably aligned with the directions of the bipolar outflows from each object detected by Grady *et al.* (2009). Interestingly, the polarization vectors of the N and S components of PDS 144 are within 15° of each other, suggesting possible co-planarity (which would still need confirmation).

On a speculative note, one cannot fail to notice that the Earth's magnetic field is connected to the Earth's rotation, with a general direction (whose sense eventually flips) close to that of our planet's angular momentum. The latter, in turn, is obviously related to, and has the memory of, the angular momentum of the primordial solar nebula's disk. If this primordial disk kept a memory of the interstellar magnetic field (such as discussed above) at the time of the formation of the Solar System, the Earth's magnetic field would provide yet another connection of our planet with the interstellar medium from where we came.

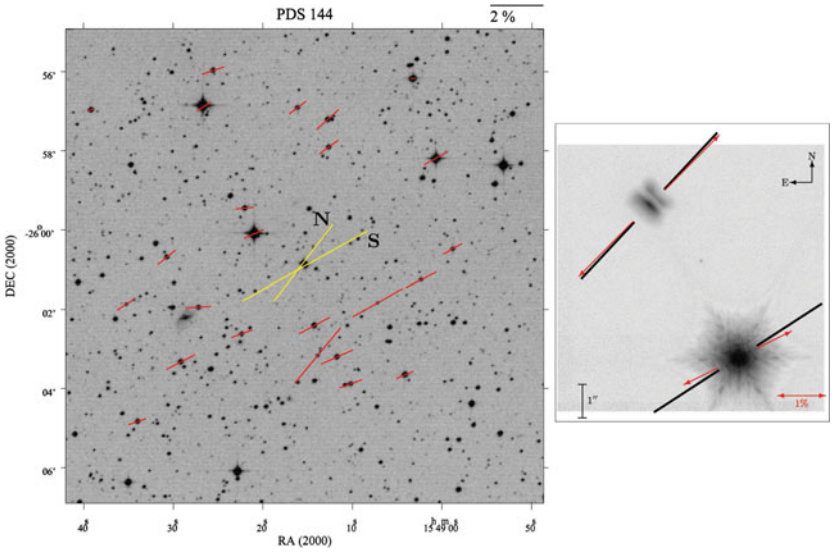

Figure 5. Left: polarization map in the V band of field stars around the PDS 144 system (red lines in the on-line version of this manuscript) plotted on a DSS2 Red image. The optical observed polarization for the binary components (N, north; S, south) is also indicated (yellow lines in the on-line version). The polarization scale is shown in the top right. Right: NIR Keck AO imaging of PDS 144 (north and south) with the PDS 144N disk resolved (adapted from Perrin *et al.* 2006). The jet axis position angles for both objects are indicated by black thick lines. The averaged intrinsic NIR polarization (H band) is also indicated (arrows). The polarization scale is indicated in the bottom right. From Pereyra, Rodrigues & Magalhães (2012).

4. The SOUTH POL survey

We close this article mentioning a forthcoming survey aimed at one of the last frontiers of astronomical surveys, that of the optical polarized sky. SOUTH POL (Magalhães *et al.* 2012) will be a survey of the Southern sky in optical polarized light. It will use a newly designed polarimetric module mounted on an 84 cm Robotic Telescope. Telescope and polarimeter are being installed at CTIO, Chile, in early 2015, with SOUTH POL being slated to start in the 2nd semester of 2015. The initial goal is to cover the sky south of declination -15^{o} in two years of observing time, aiming at a polarimetric accuracy $\leqslant$ 0.1% down to V=15, with a camera covering a field of about 2.0 square degrees.

SOUTH POL will impact areas such as Cosmology, Extragalactic Astronomy, Interstellar Medium of the Galaxy and Magellanic Clouds, Star Formation, Stellar Envelopes, Stellar explosions and Solar System, among others. In combination with other, forthcoming surveys such as GAIA, the polarization of interstellar dust should be able to provide the 3-D structure of the interstellar magnetic field of our Galaxy.

Acknowledgements

AMM would like to thank the organizers for an exciting meeting at an atractive location. His group's activities at IAG-USP are supported by São Paulo state agency FAPESP (grant no. 2010/019694-4) and Brazilian federal agencies CNPq and CAPES.

References

Bjorkman, K. S. 2006, in: M. Kraus & A. S. Miroshnichenko (eds.), *Stars with the B[e] Phenomenon*, ASP Conf. Ser. vol. 355 (San Francisco: ASP), p. 247

Bjorkman, K. S., Nordsieck, K. H., Code, A. D., Anderson, C. M., Babler, B. L., Clayton, G. C., Magalhães, A. M., Meade, M. R., Nook, M. A., Schulte-Ladbeck, R. E., Taylor, M., & Whitney, B. A. 1991, *ApJ* 383, L67

Bohren, C. F. & Huffman, D. R. 1998, *Absorption and Scattering of Light by Small Particles*, Wiley-VCH, New York

Capps, R. W., Coyne, G. V., & Dick, H. M. 1973, *ApJ* 184, 173

Carciofi, A. C. 2012, in: J. Hoffman, B. Whitney & J. Bjorkman (eds.), *Stellar Polarimetry: from Birth to Death*, ASP Conf. Ser. vol. 1429 (San Francisco: ASP), p. 121

Carciofi, A. C. & Bjorkman, J. E. 2006, *ApJ* 639, 1081.

Carciofi, A. C., Bjorkman, J. E., & Magalhães, A. M. 2004, *ApJ* 604, 238.

Carciofi, A. C., Magalhães, A. M., Leister, N. V., Bjorkman, J. E., & Levenhagen, R. S. 2007, *ApJ* 671, L49

Carciofi, A. C., Miroshnichenko, A. S., & Bjorkman, J. E. 2010, *ApJ* 721, 1079

Cassinelli, J. P., Nordsieck, K. H., & Murison, M. A. 1987, *ApJ* 317, 290

Code, A. D. & Whitney, B. 1995, *ApJ* 441, 400

Daiane, B. S., Magalhães, A. M., & Carciofi, A. C. 2015, *in preparation.*

Draine, B. T. 2011, *Physics of the Interstellar and Intergalactic Medium*, Princeton Univ. Press, Princeton

Draper, Z. H., Wisniewski, J. P., Bjorkman, K. S., Haubois, X., Carciofi, A. C., Bjorkman, J. E., Meade, M. R., & Okazaki, A. 2011, *ApJ* 728, L40

Grady, C. A., Harding, M., & Bonfield, D., *et al.* 2009, *BAAS* 41, 224

Hecht, E. 2001, *Optics*, 3rd ed. (Reading: Addison Wesley)

van de Hulst, H. C. 1981, *Light Scattering by Small Particles*, Dover, New York

Maeder, A. & Meynet, G. 2012, *Rev. Mod. Phys.* 84, 25

Magalhães, A. M. 1992, *ApJ* 398, 286

Magalhães, A. M. 2012, in: A. Carciofi & Th. Rivinius (eds.), *Circumstellar Dynamics at High Resolution*, ASP Conf. Ser. vol. 464 (San Francisco: ASP), p. 25

Magalhães, A. M., Rodrigues, C. V., Margoniner, V. E., Pereyra, A., & Heathcote, S. 1996, in: W. G. Roberge & D. C. B. Whittet (eds.), *Polarimetry of the Interstellar Medium*, ASP Conf. Ser. vol. 97 (San Francisco: ASP), p. 118

Magalhães, A. M., Pereyra, A., Melgarejo, R., de Matos, L., Carciofi, A. C., Benedito, F. F. C., Valentim, R., Vidotto, A. A., da Silva, F. N., de Souza, P. P. F., Faria, H., & Gabriel, V. S. 2005, in: A. Adamson, C. Aspin, C. J. Davis, and T. Fujiyoshi (eds.), *Astronomical Polarimetry: Current Status and Future Directions*, ASP Conf. Ser. vol. 343 (San Francisco: ASP), p. 305

Magalhães, A. M., Melgarejo, R., Pereyra, A., & Carciofi, A. C. 2006, in: M. Kraus & A. S. Miroshnichenko (eds.), *Stars with the B[e] Phenomenon*, ASP Conf. Ser. vol. 355 (San Francisco: ASP), p. 147

Magalhães, A. M., de Oliveira, C. M., Carciofi, A., Costa, R., Dal Pino, E. M. G., Diaz, M., Ferrari, T., Fernandez, C., Gomes, A. L., Marrara, L., Pereyra, A., Ribeiro, N. L., Rodrigues, C. V., Rubinho, M. S., Seriacopi, D. B., & Taylor, K. 2012, in: J. Hoffman, B. Whitney & J. Bjorkman (eds.), *Stellar Polarimetry: from Birth to Death*, ASP Conf. Ser. vol. 1429 (San Francisco: ASP), p. 244

McDavid, D. 2001, *ApJ* 553, 1027

McLean, I. S. 1979, *MNRAS* 186, 265

Melgarejo, R., Magalhães, A. M., Carciofi, A. C., & Rodrigues, C. V. 2001, *A&A* 377, 581

Mie, G. 1908, *Ann. der Physik*, Vierte Folge, Band 25, No. 3, 377

Pereyra, A., de Arajo, F. X., Magalhães, A. M., Borges Fernandes, M., & Domiciano de Souza, A. 2009, *A&A* 508, 1337

Pereyra, A., Rodrigues, C. V., & Magalhães, A. M. 2012, *A&A* 538, 59

Perrin, M. D., Duchne, G., Kalas, P., & Graham, J. R. 2006, *ApJ* 645, 1272

Rodrigues, C. V. & Magalhães, A. M. 1995, in: Karel A. van der Hucht and Peredur M. Williams (eds.), *Wolf-Rayet stars: binaries, colliding winds, evolution*, Proc. IAU Symposium no. 163 Dordrecht: Kluwer, p. 260

Rodrigues, C. V. & Magalhães, A. M. 2000, *ApJ* 540, 412

Rodrigues, C. V., Sartori, M. J., Gregorio-Hetem, J., & Magalhães, A. M. 2009, *ApJ* 698, 2031

Rybicki, G. B. & Lightman, A. P. 1975, *Radiation Processes in Astrophysics*, 2nd. ed., Wiley-VCH, New York

Serkowski, K. 1974, in: M. L. Meeks & N. P. Carleton (eds.), *Methods of Experimental Physics*, vol. 12: Astrophysics, Part A, (New York: Academic Press), p. 361

Silva, K. M. G., Rodrigues, C. V., Costa, J. E. R., de Souza, C. A., Cieslinski, D., & Hickel, G. R. 2012, *MNRAS* 432, 1587

St.-Louis, N., Moffat, A. F. J., Lapointe, L., Efimov, Yu. S., Shakhovskoj, N. M., Fox, G. K., & Piirola, V. 1993, *ApJ* 410, 342

Stephens, I. W., Looney, L. W., Kwon, W., Hull, C. L. H., Plambeck, R. L., Crutcher, R. M., Chapman, N., Novak, G., Davidson, J., Vaillancourt, J. E., Shinnaga, H., & Matthews, T. 2013, *ApJ* 769, L15

Vink, J. S., Harries, T. J., & Drew, J. E. 2005, *A&A* 430, 213

Whitney, B. A. 2011, *Bull. Astron. Soc. India* 39, p. 101

Wisniewski, J. P., Draper, Z. H., Bjorkman, K. S., Meade, M. R., Bjorkman, J. E., & Kowalski, A. F. 2010, *ApJ* 709, 1306

Wood, K., Bjorkman, K. S., & Bjorkman, J. E. 1997, *ApJ* 477, 926

Zickgraf, F. J., Wolf, B., Stahl, O., Leitherer, C., & Klare, G. 1985, *A&A* 143, 421